

**SQUEEZE FILM LUBRICATION
BETWEEN ROUGH CONICAL PLATES WITH RABINOWITSCH FLUID MODEL**

VIJAYALAXMI S. SHIGEHALLI¹, HANUMAGOWDA B N^{*2} AND RAJANI C B³

¹Department of Mathematics,
Rani Channamma University, Belagavi, India.

²School of Applied Sciences, REVA University, India.

³Department of Mathematics,
Sri Siddhartha Institute of Technology, Tumkur, India.

. (Received On: 19-09-17; Revised & Accepted On: 07-10-17)

ABSTRACT

In this paper, an analytical solution for the performance characteristics of squeeze film lubrication between rough conical plates with Rabinowitsch fluid has been studied. The modified Reynolds equation has been inferred on the basis of Christensen's stochastic model for rough surfaces. Two sorts of one-dimensional roughness patterns, viz. radial and azimuthal roughness are considered. Utilizing a small perturbation method, a closed-form result is obtained. Expressions are obtained for pressure, load carrying capacity and squeeze film time. For different operating parameter, the outcomes have been calculated. It is seen that the influence of radial (azimuthal) surface roughness pattern is to increase (decrease) the pressure, load carrying capacity and squeeze film time.

Keywords: Surface roughness, Rough conical plates, Squeeze film, Rabinowitsch fluid.

INTRODUCTION

Now a days, research on squeeze film behaviours between two approaching surfaces is observed to play a very important role in many engineering applications, such as machine tools, gears, skeletal joints, clutch plates and automotive engines. The two lubricated surfaces approaching each other with a normal velocity, phenomenon is applied to the squeeze film. The instantaneous contact among the surfaces is prevented by the thin film of lubricant contained between the surfaces. In general, the relation between the load-carrying capacity and the rate of approach is the important topic of many squeeze film studies. The squeeze-film characteristic for rectangular parallel and curved plates was studied and solutions for load carrying capacity and squeeze film time were found by Hays [1]. The performances of the squeeze films in curved circular plates was analysed by Murti [2]. Compared with the parallel plates, a higher load capacity was provided for the concave film profiles, but reverse results are found for the convex film plates. In view of different operating conditions and bearing materials, the squeeze films of different mechanisms were further explored by a number of authors, such as the spherical squeeze films by Gould [3], the porous conical plates by Prakash and Viji [4], the porous circular disks by Murti [5], between the curved annular plates by Gupta and Vora [6], on the porous circular disks by Lin [7] and the rough curved annular plates by Bujurke *et al.* [8]. All the above mentioned contributions consider the squeeze-film plates lubricated with a Newtonian lubricant. For the squeeze films operating under different severe situations, lubricating oils blended with additives of high molecular weight polymers are increasingly emphasized. The existence of these additives prevents the viscosity from varying with the temperature. These kinds of lubricants exhibit a non-Newtonian behaviour, in which the ratio between the shear stress and the rate of shear is no longer a constant. According to the experimental evidences by Wada and Hayashi [9], the non-Newtonian rheological behaviours of polymer-thickened oils can be simulated by a cubic equation model or the Rabinowitsch fluid model. In this model, the non-linear relationship between the shear stress and the shear rate is expressed as

Corresponding Author: Hanumagowda B N^{*2}
²School of Applied Sciences, REVA University, India.

$$\tau_{xy} + k\tau_{xy}^3 = \mu \frac{\partial u}{\partial y} \quad (1)$$

where the initial viscosity μ is equal to the viscosity of a Newtonian fluid and k is the coefficient of cubic stress term, the non-linear factor $k < 0$ is responsible for the property of the dilatant fluid, $k > 0$, of the pseudoplastic fluid and $k = 0$ of the Newtonian fluid. The experimental analysis of this model for the squeeze film characteristics were studied by many investigators, the parallel circular disks by Hashimoto, H. and Wada, S. [10], the parallel plane annuli by Usha and Vimala. [11], the exponential curved surfaces by Usha and Vimala [12] and also some contribution can be seen in the works on the Journal bearings studied by Sharma *et al.* [13], the slider bearings by Lin [14] and the conical bearings by Cheng-Hsing Hsu *et al.* [15].

On machine design, the surface roughness and its effects play as an important factor affecting the flow pattern and have been studied in recent times. Numerous mathematical models have been suggested to derive the various Reynolds type equations in view of the roughness effects. To analyse surface roughness effects by averaging the fluid film thickness or the flow quantities between two lubricated rough surfaces efforts have been made. In the literature, Christensen [16] proposed two sorts of one-dimensional roughness patterns-longitudinal and transverse surface roughness patterns. Several investigators have used Christensen's stochastic theory for the lubrication of rough surfaces. The performance of different bearing systems such as the squeeze film by Prakash and Toner [17], Lin *et al.* [18], Naduvanamani *et al.* [19], Wallicka[20], J.Falicki *et al.* [21] and Naduvanamani *et al.* [22].

In the present analysis, importance has been given to study the squeeze film lubrication between rough conical plates with Rabinowitsch fluid model, which has not been studied so far.

MATHEMATICAL ANALYSIS

Figure 1 illustrates the physical configuration of the squeeze film rough conical plates lubricated by a non-Newtonian fluid. The cone has an angle of 2θ and a radius of a , squeezing the fluid out of the cone housing. The film height in the direction of the cone axis is H .

The basic equations governing the flow of an incompressible non-Newtonian Rabinowitsch fluid under the assumptions of hydrodynamic lubrication for thin film is given by

$$\frac{1}{r} \frac{\partial(ru)}{\partial r} + \frac{\partial v}{\partial y} = 0 \quad (2)$$

$$\frac{\partial p}{\partial r} = \frac{\partial \tau_{xy}}{\partial y} \quad (3)$$

$$\frac{\partial p}{\partial y} = 0 \quad (4)$$

The boundary conditions assumed for velocity components are:

$$u = 0, \quad v = 0 \quad \text{at } y = 0 \quad (5a)$$

$$u = 0, \quad v = \sin \theta \frac{dH}{dt} \quad \text{at } y = H \sin \theta \quad (5b)$$

The solution for the equation (3) satisfying the cubic stress equation (1) and the boundary conditions (5a) and (5b) is

$$u = \frac{1}{\mu} \left\{ f \frac{y^2}{2} + I_1 y + k \left(f^3 \frac{y^4}{4} + f^2 y^3 I_1 + \frac{3}{2} f y^2 I_1^2 + y I_1^3 \right) \right\} + I_2 \quad (6)$$

where $f = \frac{\partial p}{\partial r}$ is the pressure gradient and $I_1 = -\frac{1}{2} f H \sin \theta$ and $I_2 = 0$ are integrating constants.

Using I_1 and I_2 in equation (6) we get

$$u = \frac{1}{\mu} \left\{ \frac{1}{2} f F_1 + k f^3 F_2 \right\} \quad (7)$$

where $F_1 = y(y - H \sin \theta)$, $F_2 = \frac{y^4}{4} - \frac{y^3 H \sin \theta}{2} + \frac{3}{8} y^2 H^2 \sin \theta - \frac{y H^3 \sin^3 \theta}{8}$.

Substituting the equation (7) and performing the integration with the associate boundary conditions, we can derive a non-linear, Reynolds equation for conical plates lubricated with Rabinowitsch fluids is obtained in the form

$$\frac{1}{r} \frac{\partial}{\partial r} \left[r \left\{ H^3 \sin^3 \theta \left(\frac{\partial p}{\partial r} \right) + \frac{3k}{20} H^5 \sin^5 \theta \left(\frac{\partial p}{\partial r} \right)^3 \right\} \right] = 12\mu \frac{dH}{dt} \sin \theta \quad (8)$$

considering $f(h_s)$ as the probability density function of the stochastic film thickness h_s and taking the stochastic average of equation (8) with respect to $f(h_s)$, we can get the averaged modified Reynolds type equation in the following form

$$\frac{1}{r} \frac{\partial}{\partial r} \left[r \left\{ E \left(H^3 \sin^3 \theta \right) \left(\frac{\partial E(p)}{\partial r} \right) + \frac{3k}{20} E \left(H^5 \sin^5 \theta \right) \left(\frac{\partial E(p)}{\partial r} \right)^3 \right\} \right] = 12\mu \frac{dH}{dt} \sin \theta \quad (9)$$

The expectancy operator $E(*)$ is defined by

$$E(*) = \int_{-\infty}^{\infty} (**) f(h_s) dh_s \quad (10)$$

where

$$f(h_s) = \begin{cases} \frac{35}{32c^7} (c^2 - h_s^2)^3, & -c < h_s < c \\ 0, & \text{elsewhere} \end{cases} \quad (11)$$

With $\sigma = c/3$ is the standard deviation.

In perspective of Christensen's stochastic theory, the analysis is done for two sorts of one-dimensional surface roughness patterns namely, radial roughness pattern and azimuthal roughness pattern.

2a. ONE-DIMENSIONAL RADIAL ROUGHNESS

The roughness striation for one-dimensional radial roughness pattern, are in the form of long narrow ridges and valleys running through r -direction (i.e. they are straight ridges and valley passing through $y=0$, $r=0$ to form star pattern), in this case the non-dimensional stochastic film thickness assumes the form $H_i = h_i + h_s(\theta, \xi)$ for $i=1, 2$ and the stochastic modified Reynolds Eq. (10) takes the form

$$\frac{1}{r} \frac{\partial}{\partial r} \left[r \left\{ E \left(H^3 \sin^3 \theta \right) \left(\frac{\partial E(p)}{\partial r} \right) + \frac{3k}{20} E \left(H^5 \sin^5 \theta \right) \left(\frac{\partial E(p)}{\partial r} \right)^3 \right\} \right] = 12\mu \frac{dH}{dt} \sin \theta \quad (12)$$

2b. ONE-DIMENSIONAL AZIMUTHAL ROUGHNESS

The roughness striation for one-dimensional azimuthal roughness pattern, is in the form of long narrow ridges and valleys running through θ -direction (i.e. they are circular ridges and valleys on the flat plate that are concentric on $y=0$, $r=0$), in this case the non-dimensional stochastic film thickness assumes the form $H_i = h_i + h_s(r, \xi)$ for $i=1, 2$ and the stochastic modified Reynolds equation (10) takes the form

$$\frac{1}{r} \frac{\partial}{\partial r} \left[r \left\{ \frac{1}{E \left(\frac{1}{H^3 \sin^3 \theta} \right)} \left(\frac{\partial E(p)}{\partial r} \right) + \frac{3k}{20} \frac{1}{E \left(\frac{1}{H^5 \sin^5 \theta} \right)} \left(\frac{\partial E(p)}{\partial r} \right)^3 \right\} \right] = 12\mu \frac{dH}{dt} \sin \theta \quad (13)$$

For an axisymmetric case, equations (12) and (13) together can be written as

$$\frac{1}{r} \frac{\partial}{\partial r} \left[r \left\{ G_1(H, \theta, c) \left(\frac{\partial E(p)}{\partial r} \right) + \frac{3k}{20} G_2(H, \theta, c) \left(\frac{\partial E(p)}{\partial r} \right)^3 \right\} \right] = 12\mu \frac{dH}{dt} \sin \theta \quad (14)$$

where

$$G_1(H, \theta, c) = \begin{cases} E(H^3 \sin^3 \theta) & \text{for radial roughness} \\ \left\{ E \left(\frac{1}{H^3 \sin^3 \theta} \right) \right\}^{-1} & \text{for azimuthal roughness} \end{cases} \quad (15a)$$

$$E\left(H^3 \sin^3 \theta\right) = \frac{35}{32c^7} \int_{-c}^c H^3 \sin^3 \theta \left(c^2 - h_s^2\right)^3 dh_s \quad (15b)$$

$$E\left(\frac{1}{H^3 \sin^3 \theta}\right) = \frac{35}{32c^7} \int_{-c}^c \frac{\left(c^2 - h_s^2\right)^3}{H^3 \sin^3 \theta} dh_s \quad (15c)$$

and

$$G_2(H, \theta, c) = \begin{cases} E\left(H^5 \sin^5 \theta\right) & \text{for radial roughness} \\ \left\{E\left(\frac{1}{H^5 \sin^5 \theta}\right)\right\}^{-1} & \text{for azimuthal roughness} \end{cases} \quad (16a)$$

$$E\left(H^5 \sin^5 \theta\right) = \frac{35}{32c^7} \int_{-c}^c H^5 \sin^5 \theta \left(c^2 - h_s^2\right)^3 dh_s \quad (16b)$$

$$E\left(\frac{1}{H^5 \sin^5 \theta}\right) = \frac{35}{32c^7} \int_{-c}^c \frac{\left(c^2 - h_s^2\right)^3}{H^5 \sin^5 \theta} dh_s \quad (16c)$$

Introducing the non-dimensional variables and parameter as follows:

$$r^* = \frac{r}{a \operatorname{Cosec} \theta}, \quad p^* = \frac{E(p) h_0^2}{\mu a \left(-\frac{dH^*}{dt}\right) \operatorname{Cosec} \theta}, \quad \beta = k \frac{\mu^2}{h_0^2 \left(-\frac{dH^*}{dt}\right)^2 \operatorname{Cosec}^2 \theta}, \quad H^* = \frac{H}{h_0}, \quad C = \frac{c}{h_0}$$

The non-linear averaged Reynolds equation and the boundary conditions for pressure in terms of non-dimensional form can be written as

$$\frac{\partial}{\partial r^*} \left[r^* \left\{ G_1^*(H^*, \theta, C) \left(\frac{\partial p^*}{\partial r^*} \right) + \frac{3}{20} \beta G_2^*(H^*, \theta, C) \left(\frac{\partial p^*}{\partial r^*} \right)^3 \right\} \right] = -1 \quad r^2 \quad (17)$$

Where β denotes the non-linear parameter responsible for the non-Newtonian effects.

It is difficult to find the exact solution for the film pressure by highly non-linear averaged Reynolds equation. To simplify the problem, we expanded the film pressure p^* based on the perturbation technique for small values of β :- $1 \ll \beta \ll +1$,

$$p^* = p_0^* + \beta p_1^* + O(\beta^2) \quad (18)$$

Substituting into the Reynolds equation (15) and leaving these second and high-order terms of β , we get the following equations for pressure p_0^* and p_1^*

$$\frac{\partial}{\partial r^*} \left[r^* \left\{ G_1^*(H^*, \theta, C) \frac{\partial p_0^*}{\partial r^*} \right\} \right] = -12r^* \quad (19)$$

$$\frac{\partial}{\partial r^*} \left[r^* \left\{ G_1^*(H^*, \theta, C) \frac{\partial p_1^*}{\partial r^*} + \frac{3}{20} G_2^*(H^*, \theta, C) \left(\frac{\partial p_0^*}{\partial r^*} \right)^3 \right\} \right] = 0 \quad (20)$$

The pressure boundary conditions are

$$\frac{dp^*}{dr^*} = 0 \quad \text{at } r^* = 0 \quad (21a)$$

$$p^* = 0 \quad \text{at } r^* = 1 \quad (21b)$$

Solving equations (19) and (20) using the boundary conditions (21a) and (21b) gives

$$p_0^* = -\frac{3(r^{*2} - 1)}{G_1^*(H^*, \theta, C)}$$

$$p_1^* = \frac{81}{10} \frac{G_2^*(H^*, \theta, C)(r^{*4} - 1)}{G_1^{*4}(H^*, \theta, C)}$$

The non-dimensional pressure $p^* = p_0^* + \beta p_1^*$ obtained in the form

$$p^* = -\frac{3(r^{*2} - 1)}{G_1^*(H^*, \theta, C)} + \frac{81\beta}{10} \frac{G_2^*(H^*, \theta, C)(r^{*4} - 1)}{G_1^{*4}(H^*, \theta, C)} \quad (22)$$

The load carrying capacity $E(W)$ is obtained in the form

$$E(W) = 2\pi \int_0^{a \cos ec \theta} r E(p) dr \quad (23)$$

The non-dimensional load carrying capacity is obtained in the form

$$W^* = 2\pi \int_0^1 r^* p^* dr^* \quad (24)$$

where

$$W^* = \frac{E(p) h_0^2}{\mu L \left(-\frac{dH^*}{dt} \right) \cos^2 \theta}$$

$$W^* = \frac{3\pi}{2G_1^*(H^*, \theta, C)} - \frac{27\pi\beta}{5} \frac{G_2^*(H^*, \theta, C)}{G_1^{*4}(H^*, \theta, C)} \quad (25)$$

The squeeze film time is obtained in the form

$$t^* = \int_{h_m=h_f}^1 \left(\frac{3\pi}{2G_1^*(H^*, C)} - \frac{27\pi\beta}{5} \frac{G_2^*(H^*, C)}{G_1^{*4}(H^*, C)} \right) dh^* \quad (26)$$

Where $t^* = \frac{E(W) h_0^2}{\mu L^4 \cos ec^2 \theta} t$

RESULTS AND DISCUSSION

In the present analysis and solutions, the effect of surface roughness pattern on the squeeze film lubrication between rough conical plates with Rabinowitsch fluid is analysed. The results are analysed for various non-dimensional parameters.

Pressure

Figure2 depicts the variation of non-dimensional pressure p^* with r^* for various values of β with $h^* = 0.4$, $C = 0.3$ and under the half cone angle $\theta = \pi/3$ for radial and azimuthal roughness patterns and it is seen that the non-dimensional pressure decreases with increasing values of r^* and β .

Figure3 shows the variation of non-dimensional pressure p^* with r^* for various values of C with $\theta = \pi/3$, $\beta = 0.001$ and $h^* = 0.4$ for both types of roughness patterns. It is seen that the non-dimensional pressure decreases for radial roughness and increases for azimuthal roughness pattern with increasing values of r^* and C .

Figure4 depicts the variation of non-dimensional pressure p^* with r^* for various values of θ with $h^* = 0.4$, $\beta = 0.001$ and $C = 0.2$ for both roughness patterns. It is clear from the figure that, the non-dimensional pressure decreases with increasing values of r^* and β for both roughness patterns.

Load carrying capacity

The variation of non-dimensional load carrying capacity W^* with film thickness h^* for different values of non-linear factor β with $\theta = \pi/3$ and $C = 0.2$ is as shown in Figure5 for both radial and azimuthal roughness patterns. It is seen that, the load carrying capacity W^* decreases for increasing values of h^* for both radial and azimuthal roughness patterns.

Figure6 depicts the variation of non-dimensional load carrying capacity W^* with h^* for different values of roughness parameter C with $\beta = 0.001$ and $\theta = \pi/3$. In both type of roughness patterns it is observed that, W^* decreases for increasing values of h^* and C for radial roughness and increases for azimuthal roughness patterns.

Figure7 shows the variation of non-dimensional load carrying capacity W^* with h^* for different values of θ with fixed values of roughness parameter $C = 0.2$ and $\beta = 0.001$ for both types of roughness patterns. It is observed that W^* increases for radial roughness and decreases for azimuthal roughness patterns.

Squeeze film time

Figure 8 shows the variation of squeeze film time t^* with film thickness h_f^* for different values of non-linear factor β with fixed values of roughness parameter $C = 0.2$ and $\theta = \pi/3$. In both radial and azimuthal roughness patterns it is seen that, the response time t^* increases with increasing values of h_f^* and β .

Figure 9 depicts the variation of squeeze film time t^* with film thickness h_f^* for different values of C and $\beta = 0.001$ for both types of roughness parameter. It is observed that the squeeze film time decreases for radial roughness and increases for azimuthal roughness pattern with increasing values of h_f^* and C .

The variation of non-dimensional squeeze film time t^* with film thickness h_f^* for different values of θ with $C = 0.2$ and $\beta = 0.001$ is as shown in the Figure10. It is seen that the t^* decreases (increases) for radial (azimuthal) roughness pattern with increasing values of h_f^* and C .

CONCLUSIONS

The influence of surface roughness and its effects on squeeze film characteristics between rough conical plates with Rabinowitsch fluid is presented in this paper. For both roughness patterns, the averaged modified Reynolds equations are derived. By using a small perturbation technique, the non-linear Reynolds equations are solved. According to the analysis and the results discussed and presented in the above section, the following conclusions have been considered.

- It is seen that for the rough conical plates, the non-dimensional pressure, non-dimensional load carrying capacity and squeeze film time decreases with increasing value of non-linear factor β .
- In the presence of a Rabinowitsch fluid, one-dimensional azimuthal surface roughness pattern on the rough conical plates improves the squeeze film characteristics whereas the performance of the squeeze film decline due to the presence of radial surface roughness pattern.

NOMENCLATURE

a	cone radius
a^*	non-dimensional radius of the cone
β	non-dimensional non-linear factor of lubricants
C	non-dimensional roughness parameter
E	expectancy operator
h_s	stochastic film thickness
H_i	film thickness
H	non-dimensional film thickness
p	pressure in the film region
p^*	non-dimensional pressure in the film region
θ	half cone angle
r, θ	radial and axial coordinates
x, y	horizontal and vertical coordinates
t	time of approach
t^*	non-dimensional time of approach
V	squeezing film velocity
u, w	velocity components of lubricant in the x and y directions, respectively

W	the load carrying capacity
W^*	non-dimensional load carrying capacity
μ	initial viscosity
k	non-linear factor of lubricants
τ_{xy}	shear stress component

REFERENCES

1. Hays D.F., Squeeze film for rectangular plates, ASME Journal of Basic Engineering, 85, (1963), 243-246.
2. Murti P.R.K., Squeeze film for curved circular plates, ASME Journal of Lubrication Technology, 97, (1975), 650-652.
3. Gould P., High pressure spherical squeeze films, ASME Journal of Lubrication Technology, 93, (1971), 207-208.
4. Prakash J., Viji S.K., Load capacity and time –height relations for squeeze film between porous plates, Wear, 24, (1973), 309-322.
5. Murti P.R.K., Squeeze film behavior in porous circular disks, ASME Journal of Lubrication Technology, 96, (1974), 206-209.
6. Gupta J.L., Vora, K.H., Analysis of squeeze films between curved annular plates, ASME Journal of Lubrication Technology, 102, (1980), 48-50.
7. Lin J.R., Viscous shear effects on the squeeze film behaviour on porous circular disks, International Journal of Mechanical Sciences, 39, (1980), 373-384.
8. Burjurke N.M., Naduvinamani N.B., Basti D.P., Effect of surface roughness on the squeeze film lubrication between curved annular plates”, Industrial Lubrication and Tribology, 59, (2007), 178-185.
9. Wada S., Hayashi H., Hydrodynamic lubrication of journal bearings by pseudo-plastic lubricants(part 2, experimental studies), Bulletin of the JSME, 14, (1971), 279-286
10. Hashimoto H., Wada S., The effects of fluid inertia forces in parallel circular squeeze film bearing lubricated with pseudoplastic fluids, ASME-Journal of Tribology, 108, (1986), 282-287.
11. Usha R., Vimala P., Fluid inertia effects in a non-Newtonian squeeze film between two plane annuli, ASME Journal of Tribology, 122, (2000), 872-875.
12. Usha R., Vimala P., Inertia effects in a curved non-Newtonian squeeze film, ASME Journal of Applied Mechanics, 68, (2001), 944-948.
13. Sharma S.C., Jain S.C., Sah P.L., Effect of non-Newtonian behaviour of lubricant and bearing flexibility on the performance of slot-entry journal bearing, Tribology International, 33, (2000), 505-517.
14. Lin J.R., on-Newtonian effects on the dynamic characteristics of one-dimensional slider bearings: Rabinowitsch fluid model, Tribology Letters, 10, (2001), 237-243.
15. Cheng-Hsing Hsu., Jaw-Ren Lin., Lian-Jong Mou., Chia-Chuan Kuo., Squeeze film characteristics of conical bearings operating with non-Newtonian lubricants-Rabinowitsch fluid model, Industrial Lubrication and Tribology, 66, (2014), 373-378.
16. Christensen H., Stochastic Models for Hydrodynamic Lubrication of Rough Surface, Proceedings of the Institution of Mechanical Engineers, Part J: Journal of Engineering Tribology, 184, (1969), 1013-102.
17. Prakash J., Toner K., Roughness effects in circular squeeze plates, ASLE Trans, 20, (1977), 257.
18. Lin J.R., Hsu C.H., Lai C., Surface roughness effects on the oscillating squeeze film behaviour of long partial journal bearings”, Comp. and Str., 80, (2002), 297.
19. Naduvinamani N.B., Hiremath P.S., Gurubasavaraj G., Effect of surface roughness on the static characteristics of rotor bearings with couple stress fluids, Comp. and Str., 80, (2002), 1243.
20. Wallicka A., Walicki E., Jurczak P., Falicki J., Curvilinear squeeze film bearing with rough surfaces lubricated by a Rabinowitsch-Rotem-Shinnar fluid, Applied Mathematical Modelling, (2016), 1-12.
21. Wallicka A., Porous curvilinear squeeze film bearing with rough surfaces lubricated by a power-law fluid, J. Porous Media, 15 (1), (2012), 29-49.
22. Naduvinamani N.B., Hanumagowda B.N., Syeda Tasneem Fathima., Combined effects of MHD and surface roughness on couple-stress squeeze film lubrication between porous circular stepped plates, (2012), 56, 19-29.
23. Hamrock B. J., Fundamentals of Fluid Film Lubrication, McGraw-Hill, New York, NY, (1994).

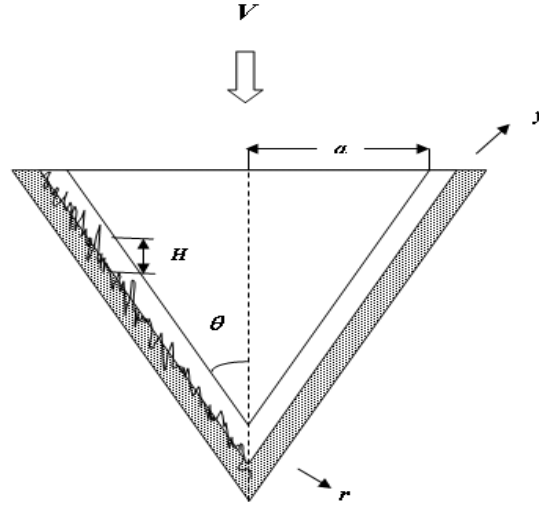


Figure-1: Physical configuration of squeeze film rough conical plates lubricated with Rabinowitsch Fluid.

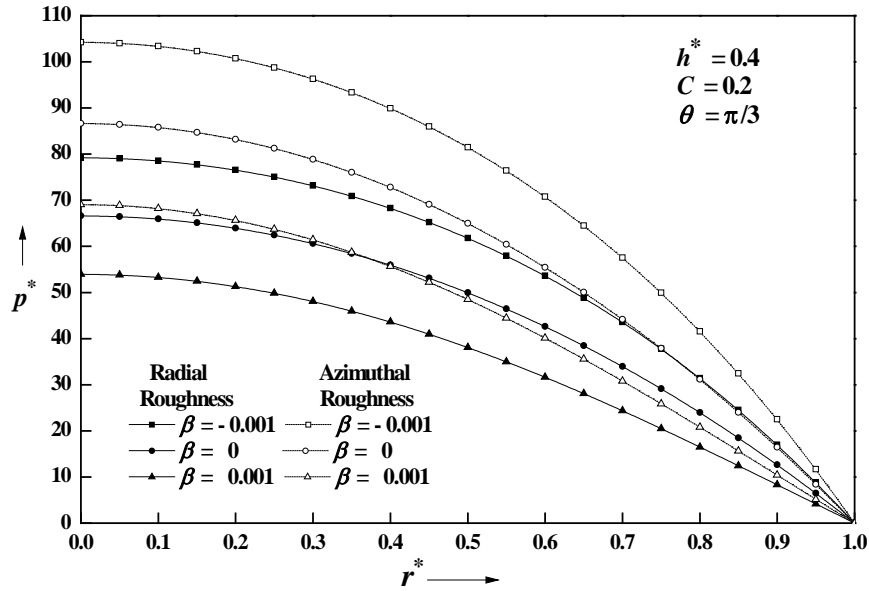


Figure-2: Variation of non-dimensional pressure p^* with r^* for different values of β with $h^* = 0.4$, $C = 0.3$ and $\theta = \pi/3$

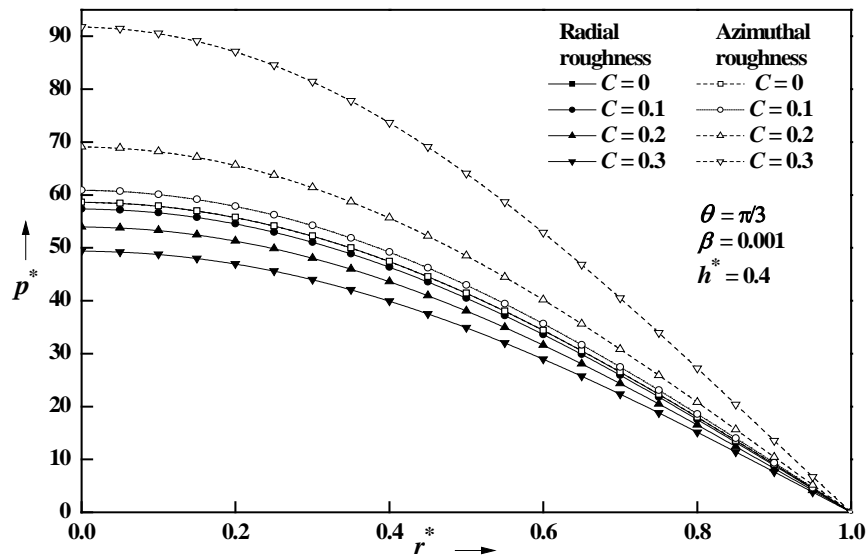


Figure-3: Variation of non-dimensional pressure p^* with r^* for different values of C with $\theta = \pi/3$, $\beta = 0.001$ and $h^* = 0.4$

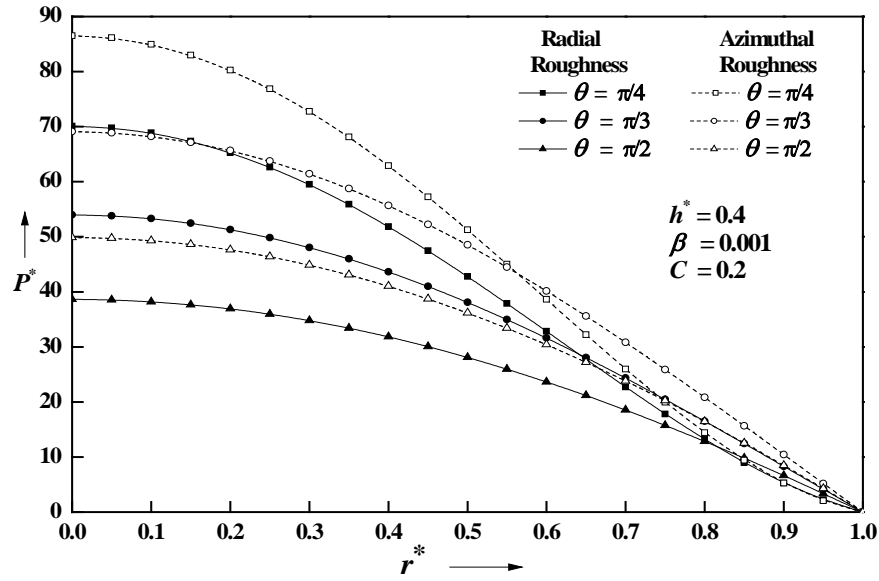


Figure-4: Variation of non-dimensional pressure p^* with r^* for different values of θ with $h^* = 0.4$, $\beta = 0.001$ and $C = 0.2$

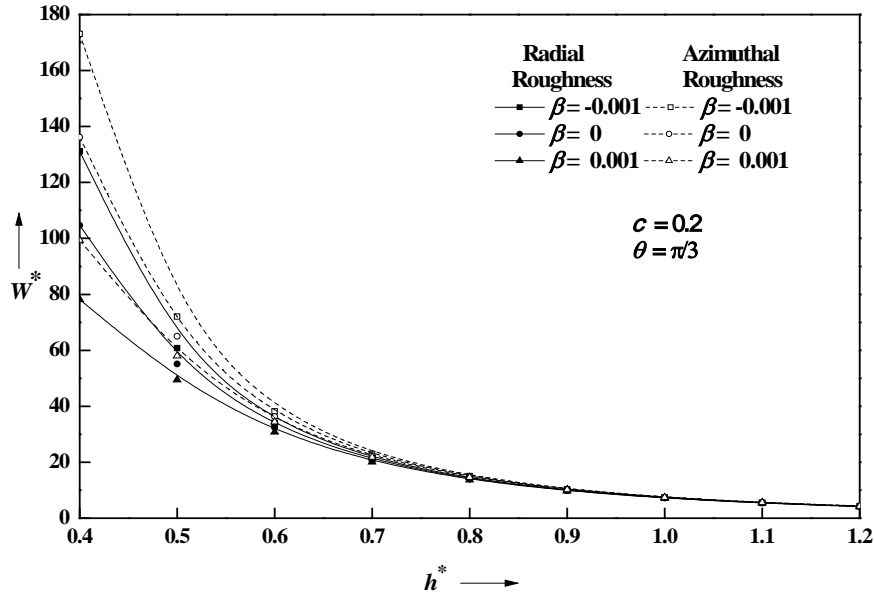


Figure-5: Variation of non-dimensional load carrying capacity w^* with film thickness h^* for different values of β with $\theta = \pi/3$ and $C = 0.2$

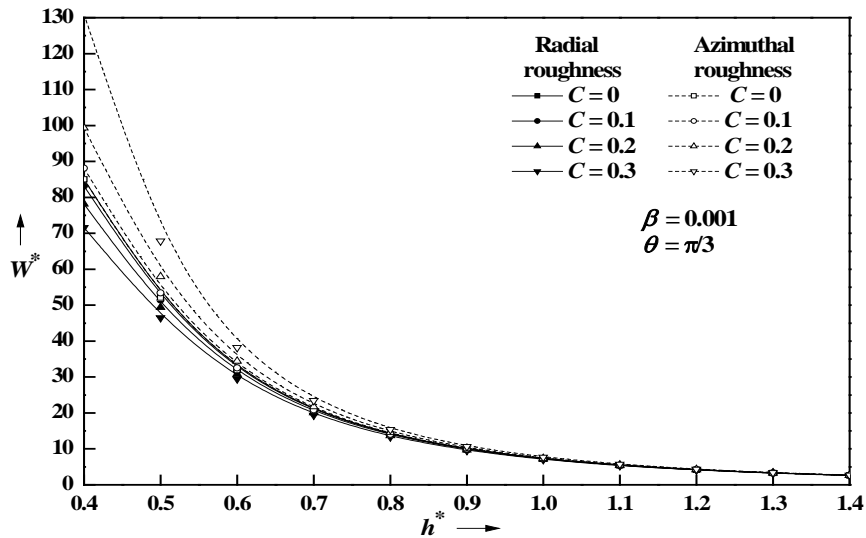


Figure-6: Variation of non-dimensional load carrying capacity W^* with film thickness h^* for different values of C with $\beta = 0.001$ and $\theta = \pi/3$

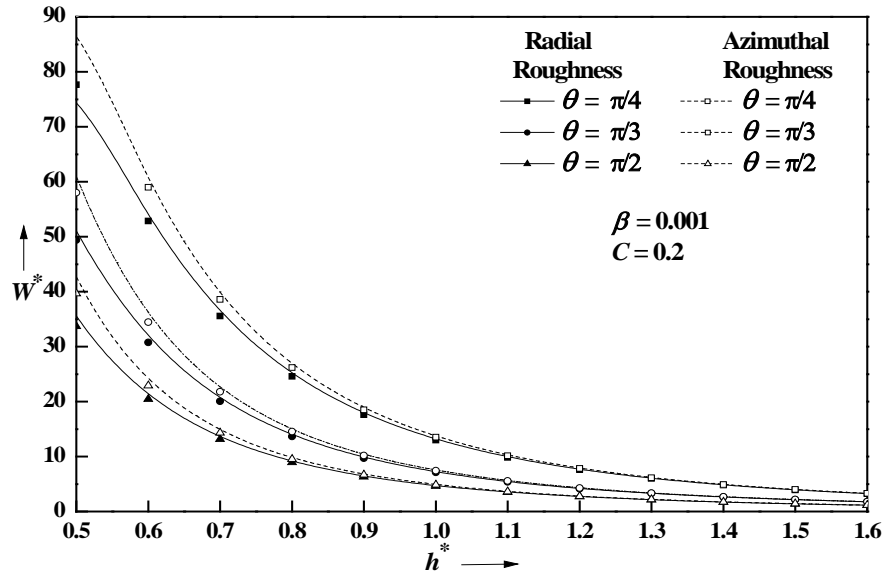


Figure-7: Variation of non-dimensional load carrying capacity W^* with film thickness h^* for different values of θ with $\beta = 0.001$ and $C = 0.2$

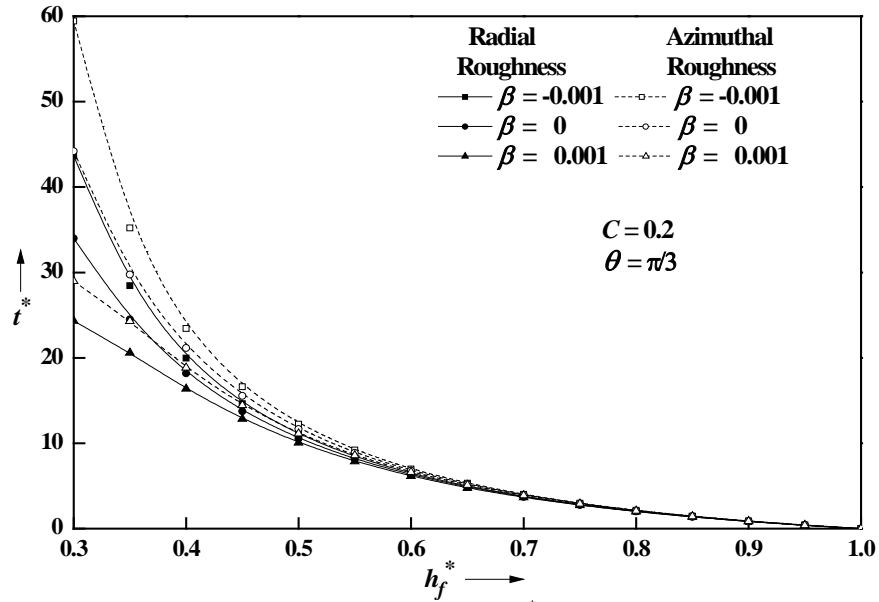


Figure-8: Variation of squeeze film time t^* with film thickness h_f^* for different values of β with $C = 0.2$ and $\theta = \pi/3$

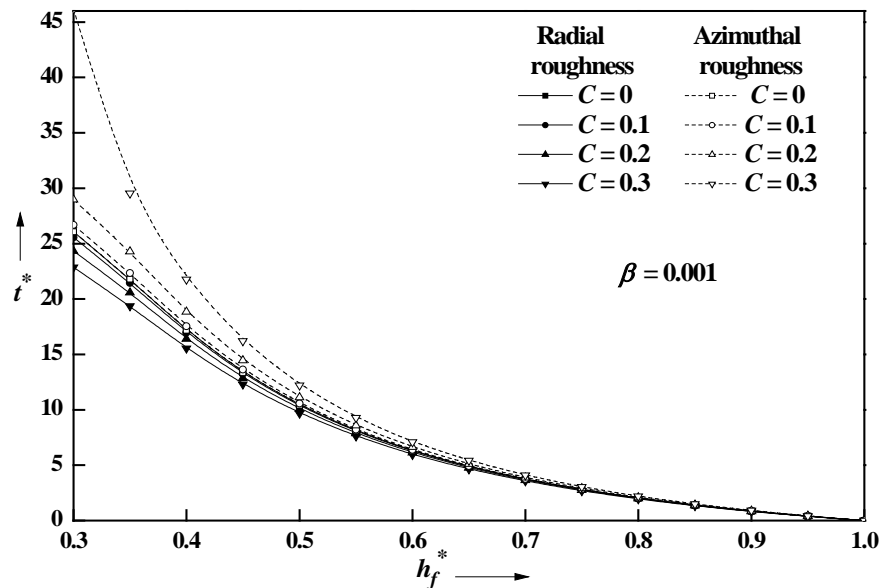


Figure-9: Variation of squeeze film time t^* with film thickness h_f^* for different values of C and $\beta = 0.001$

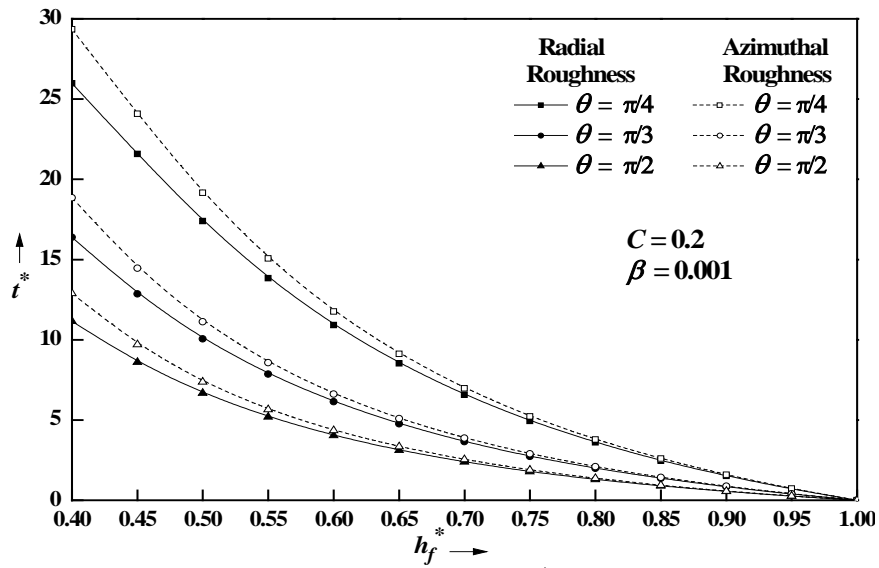


Figure-10: Variation of squeeze film time t^* with film thickness h_f^* for different values of θ $C = 0.2$ and $\beta = 0.001$

Source of support: Nil, Conflict of interest: None Declared.

[Copy right © 2017. This is an Open Access article distributed under the terms of the International Journal of Mathematical Archive (IJMA), which permits unrestricted use, distribution, and reproduction in any medium, provided the original work is properly cited.]